The Use of Variable Density Self-Assembled Monolayers to Probe the Structure of a Target Molecule

Cynthia Bamdad
Committee for Higher Degrees in Biophysics, Harvard University, Cambridge, Massachusetts 02138 USA

ABSTRACT VP16, a protein encoded by herpes simplex virus, has a well-characterized 78 amino acid acidic activation domain. When tethered to DNA, tandem repeats of an eight amino acid motif taken from this region stimulate the transcription of a nearby gene. This work addresses how these minimal activation motifs interact with a putative target, the general transcription factor TATA box binding protein (TBP), and the biological relevance of this mechanism of action. I developed novel biophysical techniques to discriminate among three possible mechanistic models that describe how reiterated peptide motifs could synergistically effect transcription: 1) the peptide motifs simultaneously bind to quasi-identical sites on TBP, producing a high-affinity bivalent interaction that holds the general transcription factor near the start site of transcription; 2) the binding of one recognition motif causes an allosteric effect that enhances the subsequent binding of additional peptide motifs; or 3) a high-affinity interaction between the peptide repeats and TBP does occur, but rather than being the result of a "bivalent" interaction, it results from the summation of multiple interactions between the target protein and the entire length of the peptide. I generated self-assembled monolayers (SAMs) that presented different densities of the activation motif peptide in a two-dimensional array to test for avidity effects. Surface plasmon resonance (SPR) was used to measure the amount of target (TBP) binding as a function of the peptide density; a marked increase in avidity above a characteristic, critical peptide surface density was found. Competitive inhibition experiments were performed to compare the avidity of peptide motifs, tandemly repeated two or four times, and single motifs separated by a flexible linker. Four iterations of the motif, preincubated with TBP, inhibited its binding to high-density peptide surfaces ~250-fold better than two iterations. Single peptide motifs joined by a flexible amino acid linker inhibited TBP binding to surface peptide nearly as well as four tandem repeats. The results favor mechanistic model 1: reiterated activation motifs interact with TBP through a high-affinity interaction that is the result of the cooperative effect of single motifs simultaneously binding to separate sites on TBP. This finding is consistent with the idea that DNA-bound activation domains trigger the transcription of a nearby gene by tethering the general transcription factor, TBP, near the start site of transcription.

INTRODUCTION

Self-assembled monolayer (SAM) biosensor chips were engineered to present different surface densities of peptides to target molecules in solution. SAMs were chosen for peptide immobilization because they are highly ordered two-dimensional (2D) arrays that allowed for the controlled spacing and orientation of peptides.

Alkane thiolates spontaneously self-assemble onto gold substrates, from solution, to form uniform monolayers. Studies indicate that the sulfurs deposit on the gold in a defined hexagonal tiling pattern while the alkyl chains pack, due to hydrophobic forces, to form a highly ordered crystalline-like matrix (Nuzzo et al., 1990). The pioneering work of Whitesides and colleagues (Pale-Grosdamange et al., 1991) showed that alkane thiolates, terminated with bulky headgroups, could form SAMs without disrupting the underlying order of the packed carbon chains. We recently reported (Bamdad et al., 1994; Sigal et al., 1996) the generation of a mixed species SAM that incorporated a Ni(II) chelating group [nitrilotriacetic acid (NTA) (Hochuli et al., 1987)] for the specific capture of histidine-tagged proteins. This paper describes how the density of NTA in the 2D SAM was varied to present different densities of histidine-tagged peptides to probe the binding site(s) of a target molecule, TATA box binding protein (TBP). The objective of this work was to determine the feasibility of 1) using variable density peptide surfaces to determine the "valency" of a target molecule by seeking a kinetic difference between monovalent and bivalent binding, and 2) extrapolating an interbinding site distance on the target molecule by calculating an average distance between peptides on the surface. We imagine that this kind of structural information about a target molecule (previously only available by difficult and time-consuming structure determination) could be valuable for the design of high-affinity bivalent drugs.

Variable-density NTA-SAMs were used to probe the binding site(s) of a biologically important molecule, the human general transcription factor TATA box-binding protein (hTBP) (reviewed by Burley and Roeder, 1996). hTBP has been implicated as a direct target of transcriptional activators such as VP16 (Ingles et al., 1991); in fact, the need for an activator is eliminated when TBP is artificially tethered to a DNA promoter (Xiao et al., 1995). Transcriptional activator proteins are modular in that they have functionally separable domains (Brent and Ptashne, 1985): a

Received for publication 11 July 1997 and in final form 1 July 1998.

Address reprint requests to Dr. Cynthia Bamdad, CMS, 101 Waverly Drive, Pasadena, CA 91105. Tel.: 626-584-5900 ext. 23; Fax: 626-584-0909; E-mail: monopole@rocketmail.com.

© 1998 by the Biophysical Society

0006-3495/98/10/1989/08 $2.00

DNA binding domain and an activating region. The structures of TBP (Nikolov et al., 1995) and several activator DNA binding domains (Marmorstein et al., 1992; Ellenberger et al., 1992; Baleja et al., 1992) have been solved, yet the structure of an activating region, alone or complexed with a target molecule, has remained elusive. Fundamental questions as to *how* an activating region effects gene transcription remain unanswered. One mechanistic model of gene activation proposes that DNA-bound activators trigger transcription by merely "recruiting" some necessary factor, perhaps TBP, to the promoter through direct contact with the activating region (Triezenberg, 1995). Another model proposes that activating regions induce a conformational change in a target protein(s) (Sheldon and Reinberg, 1995) or sequentially perform some function until a threshold is reached that catalyzes gene transcription.

An interesting observation is that in eukaryotes, more than one DNA-tethered activator is typically required to achieve activated transcription and that multiply bound activators transcribe synergistically (Lin et al., 1990). Cryptic repeats of minimal activation motifs have been identified in eukaryotic activators that, when tandemly reiterated and tethered to DNA, efficiently activate transcription in vitro (Tanaka and Herr, 1994). An eight amino acid minimal activation motif (DFDLDMLG) derived from the prototypic mammalian activator VP16 was recently identified (Tanaka, 1996). This research used novel biophysical methods to quantitate the kinetics, as well as investigate the mechanism, of the interaction between hTBP and tandem repeats of the VP16 minimal motif.

The interactions were characterized by surface plasmon resonance (SPR) in a BIAcore instrument. SPR is a fairly new optical technique for the real-time detection and kinetic analysis of intermolecular interactions (Liedberg et al., 1983; Daniels et al., 1988; Löfås and Johnsson, 1990). The basis of the technology is as follows: ligands are immobilized on a surface; putative target molecules are flowed over this surface; the protein concentration at the solution surface interface changes as the target binds the ligand. The increased protein mass at the interface causes a change in the optical properties of the system. The amount of new protein recruited to the interfacial region can be quantitated by measuring the change in the angle at which light reflected off the interface is a minimum (for a review see Bamdad, 1997). Changes in this angle are measured in resonance units (RU) where 1 RU is defined as a change of 1/10,000 of a degree. A rule of thumb is that for a distance of ~150 nm from the interface, 1 ng protein/mm^2 registers 10^3 RU.

SAMs that incorporated an NTA group for the specific binding of histidine-tagged peptides were generated. The density of NTA in the SAM was varied so that different amounts of a histidine (His)-tagged activation motif could be presented to TBP in solution. SPR was used to quantitate avidity effects between TBP and surface-bound peptides as a function of peptide density.

METHODS

Protein preparation

hTBPc was prepared according to Nikolov et al. (1996) and full-length His-tagged hTBP according to Lee et al. (1991). Glutathione S-transferase (GST) fusion proteins were prepared according to Tanaka (1996). The preparation of Gal-4–VP16 is described by Hori et al. (1995).

DNA

TATA sequence DNA was prepared according to Parvin et al. (1995), and TATA-37 was prepared with the exception that it was not circularized. A 50-bp double-stranded oligo containing two Gal-4 binding sites, synthesized and quantitated by GibcoBRL (Life Technologies Inc., Grand Island, NY), was used as nonspecific control DNA. Equal mass amounts of specific versus nonspecific DNA were added.

Synthetic peptides

Peptides were obtained from the Biopolymers Facility, Department of Biological Chemistry and Molecular Pharmacology, Harvard Medical School, Boston, MA. They were generated by F-MOC synthesis and quantitated by amino acid analysis, analytical HPLC, and mass spectroscopy.

Preparation of self-assembled monolayers

NTA-SAM were prepared according to Sigal et al. (1996). A panel of incrementally different density NTA surfaces was generated by serial dilution of a stock solution containing 11.4% NTA-thiol, relative to triethylene glycol-terminated thiol, into solutions containing the triethylene glycol-terminated thiol alone. Total thiol concentration was kept constant at 1 mM. NTA-SAM were stored under argon for up to 1 week before use. Background levels of binding were assessed by passing reactants over underivatized GST surfaces and subtracted.

Surface plasmon resonance

Experiments were carried out in a BIAcore instrument (Biacore AB, Uppsala, Sweden) at room temperature in phosphate buffered saline (PBS) (137 mM NaCl) running at a constant flow rate of 5 μl/min. Sample injection volumes (plugs) were 35 μl. Association and dissociation rate constants were extracted from the data with BIAevaluation software, version 2.1, assuming a pseudo-first-order kinetics model: $A + B \rightleftharpoons AB$. Error rates were taken from the deviation of measurements among multiple experiments performed on surfaces of different NTA densities with a range of protein concentrations and using several different protein preparations, of the same species, to account for variation of the active concentration of a component.

Statistical calculations

Sulfur atoms bind to gold to form a face-centered hexagonal tiling pattern 4.99 Å on edge (Ulman, 1966). We assume that in an ordered monolayer all the positions of the hexagon are occupied by a thiol. Each vertex is shared by three hexagons, so there are three possible positions for thiol deposition per hexagon. If the thiol solution is doped with a derivatized species of thiol, such as ours is, the average number of NTA-thiols deposited per some number of hexagons (λ), can be calculated, assuming Poisson statistics, for a given NTA-thiol concentration. (It was assumed that the concentration of NTA-thiol in solution was equal to its concentration in the SAM; see Fig. 2 of Sigal et al., 1996). The equation in Fig. 1 calculates how many hexagons, on average, must be filled before two NTA- thiols are deposited. For a 3.8% NTA-thiol concentration in solution, relative to EG_3-thiol, an average of 17.5 hexagons must be filled before two

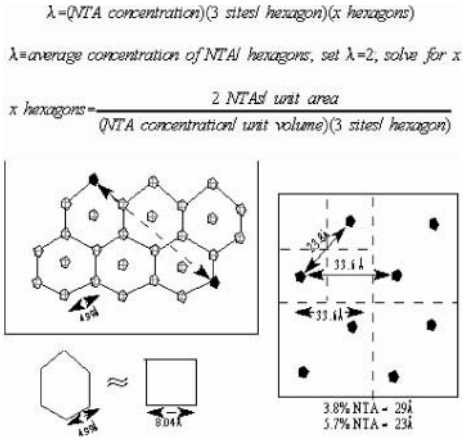

FIGURE 1 Mixed SAMs were generated by doping a thiol solution with an NTA-terminated thiol (designed to capture His-tagged proteins). Sulfur atoms deposit on gold substrates in a hexagonal tiling pattern 4.99 Å on edge with three possible positions for thiol deposition per hexagon. If we assume that in a well-ordered SAM all sites are occupied, we can calculate from Poisson statistics an average distance between NTA-thiols for a given NTA concentration. The equation calculates how many hexagons must be filled before two NTA-thiols are deposited. For a 3.8% NTA-thiol concentration in solution, relative to EG_3-thiol, an average of 17.5 hexagons must be filled before two NTA ligands appear. For a 5.7% NTA solution, 11.7 hexagons must be filled before an average of two NTA ligands are deposited. The area of a hexagon 4.99 Å on edge is 64.69 $Å^2$, which is equal to the area of a square, 8.04 Å on edge. NTA ligands on SAM formed from a 3.8% NTA-thiol solution would be an average of 29 Å apart, while NTA ligands in a SAM formed from a 5.7% NTA-thiol solution would be 23 Å apart. (It was assumed that the concentration of NTA-thiol in solution was equal to its concentration in the SAM; see Fig. 2 of Sigal et al., 1996).

NTA ligands appear. For a 5.7% NTA solution, 11.7 hexagons must be filled before an average of two NTA ligands are deposited. The area of a hexagon 4.99 Å on edge is 64.69 $Å^2$, which is equal to the area of a square 8.04 Å on edge; 17.5 hexagons would occupy the same area as a square $(17.5 \times 8.04^2)^{1/2}$ Å on edge, which equals 33.6 Å. Two NTA ligands were arbitrarily placed in a square representing 17.5 hexagons either 33.6 Å or 23.8 Å apart (see Fig. 1). We argue that since there are equal numbers of nearest and next-nearest neighbors, the average of these two distances is a first-order approximation of the average distance between ligands resulting from a random distribution. According to this model, NTA ligands on SAM formed from a 3.8% NTA-thiol solution would be an average of 29 Å apart, while NTA ligands in a SAM formed from a 5.7% NTA-thiol solution would be 23 Å apart. Calculations were done to evaluate the contribution of clustering using Poisson statistics. Equation 1 calculates the probability, P, of having n NTA ligands per unit area, where λ equals the average number of NTA per unit area. Equation 2 calculates the ratio of the probabilities of having one NTA ligand to two NTA ligands deposited per unit area. It is 17 times more likely to get one NTA than two, per unit area, for 3.8% NTA-thiol SAM and 11 times more likely at 5.7% NTA concentration.

$$P(n) = e^{-\lambda}\lambda^n/n! \tag{1}$$

$$\frac{P(1)}{P(2)} = \frac{e^{-(3\ \text{sites})([0.038]\text{NTA})}[(3)(0.038)]^1/1!}{e^{-(3\ \text{sites})([0.038]\text{NTA})}[(3)(0.038)]^2/2!} \tag{2}$$

RESULTS

A panel of variable-density NTA-SAMs were prepared by diluting the concentration of the active component, NTA-thiol, relative to that of the inert component, EG_3-thiol, in ethanol solutions. Gold-coated glass slides were incubated in solutions containing 1.3%, 3.8%, 5.7%, or 11.4% NTA-thiol, with the total thiol concentration constant at 1 mM. The SAMs were glued onto blank CM-5 SPR chip cassettes and docked into a BIAcore instrument. A 16-mer peptide comprised of two repeats of the eight amino acid minimal activation motif (DFDLDMLG X), derived from the human activator VP16, was fused to His-tagged GST (GST-2X). The fusion proteins were then immobilized on variable-density SAMs through complexation of the NTA group by the protein's His tag. This generated a series of surfaces that displayed peptides at incrementally decreasing distances from each other. The core region of human TBP (hTBPc: residues 155–335) (Nikolov et al., 1996) was injected over the peptide surfaces. GST-2X immobilized at low density (1.3–3.8%), was unable to bind hTBPc. In contrast, when the same concentration hTBPc was injected over a more dense (5.7–11.4%) GST-2X surface, where the average distance between peptide motifs would be smaller, a high-affinity interaction resulted (see Fig. 2 and Table 1). As a control, fusion proteins bearing four iterations of the minimal motif (GST-4X) were immobilized on the different density SAMs and assayed for the ability to bind the target molecule. Human TBPc, in solution, bound identically to GST-4X surfaces irrespective of the peptide density (see Fig. 3 and Table 1). As the graph of Fig. 4 shows, the stoichiometry of hTBPc binding to GST-4X derivatized surfaces is a constant, independent of the immobilization density. In contrast, the binding of hTBPc to GST-2X surfaces is a nonlinear function of the surface density. Notably, at corresponding surface concentrations, GST-2X bound half as much hTBPc as GST-4X, suggesting that two 2X modules immobilized at close proximity to each other (high density) simultaneously contact one hTBPc molecule. Kinetic rate constants were extracted by analyzing association and dissociation phases of sensorgram curves using a nonlinear regression curve fitting program: BIAevaluation 2.1 (Biacore AB). The analysis assumed pseudo-first-order reactions. The interaction between GST-4X and hTBPc was characterized by an average association rate of 2.5×10^4 s^{-1} M^{-1} and an average dissociation rate of 4×10^{-4} s^{-1}, yielding a calculated average k_D of 16×10^{-9} M. Standard errors obtained for each SPR experiment were considerably smaller than the variation in kinetic rates measured among several experiments using a wide range of NTA concentrations. There could be as much as a twofold variation in the calculated k_D.

Sensorgram association curves from the binding of hTBPc to GST-2X could not be fit by pseudo-first-order kinetics, again consistent with the idea that two 2X modules bind one hTBPc molecule. However, the dissociation phase of the sensorgram was well fit and yielded an average k_d of $1.5 \times 10^{-3} \pm 0.13$ s^{-1} for the interaction. The almost 10-fold difference between the 4X k_d and 2X k_d may indicate that the 2X dissociation curve is the superposition of two decay rates, corresponding to two dissociating species.

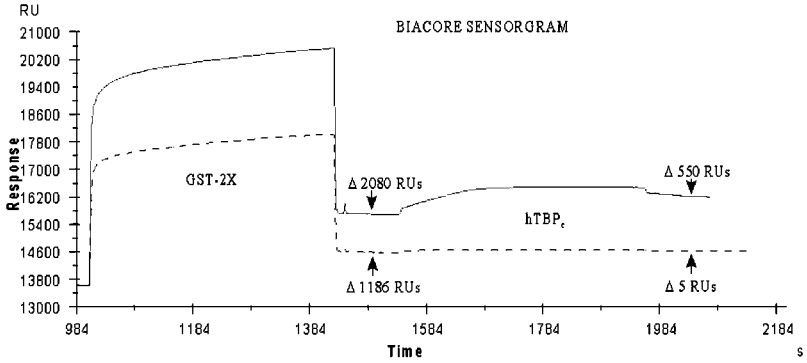

FIGURE 2 hTBPc in solution will not bind to GST-2X peptide surfaces unless peptides are immobilized close to one another. The BIAcore SPR instrument records changes in the angle of minimum reflectance (RU) as a function of time. Reagents are flowed over individual flow cells of the SAM. The "square waves" represent injections of protein "plugs" that interrupt the constant buffer flow. An association constant can be derived from an analysis of the initial phase of the injection and a dissociation rate can be extracted from analysis of the system as it returns to buffer flow. GST-2X or -4X fusion proteins (X = DFDLDMLG) were separately immobilized on NTA-SAMs via His-tags, then hTBPc [124 nM] was injected over the surfaces. An overlay of two SPR sensorgrams shows that hTBPc does not bind to GST-2X immobilized on a 3.8% NTA-SAM (*dashed line*), but binds very tightly when immobilized on a 5.7% NTA-SAM (*solid line*).

We speculated that, at high NTA density, the chip surface acted as a rigid linker between two 2X modules to mimic a 4X module, thus creating a higher affinity ligand. Three possible models might explain why the 4X peptide is a higher affinity ligand for hTBPc than a 2X peptide (Fig. 5). Model 1 proposes that the 4X peptide is a "bivalent" ligand that simultaneously and cooperatively binds more than one site on the target protein, producing a high-affinity interaction characterized by a slower off-rate (Jencks, 1981). Model 2 says the binding of one recognition motif causes an allosteric effect that enhances the binding of subsequent motifs. Four connected minimal motifs provide for an increased local concentration of ligand available for the second higher-affinity interaction. Model 3 proposes that the higher-affinity interaction is the result of the summation of multiple interactions of equal strength between the target protein and the entire length of the peptide. A prediction of Model 1 is that 2X peptides, free in solution, will interact with hTBPc independently and exhibit a faster off-rate, which is characteristic of monovalent binding. Therefore, if hTBPc is pre-bound by peptide in solution, the 4X peptide should be a much better inhibitor of hTBPc binding to surface immobilized ligand than the 2X peptide. Model 2 predicts that hTBPc pre-bound by 4X or 2X peptides (at twice the concentration) would be similarly inhibited, so long as incubation concentrations were high enough to compensate for the 4X "local concentration advantage." Model 3 implies that mutation of amino acids within the peptide would decrease its affinity for TBP as an approximately linear function of the number of mutations.

In order to compare dissociation rates, aliquots of hTBPc were preincubated at very high concentration (35 μM) with either buffer, 2X peptide (1:4 stoichiometry), or 4X peptide (1:2 stoichiometry), then diluted to the usual hTBP$_c$ concentration (124 nM) before injection over GST-4X surfaces. Synthetic 2X (16-mer) and 4X (32-mer) peptides were used to eliminate possible interference from GST. Table 2 shows that the preincubation of hTBPc with 2X peptide was in no way inhibitory to its interaction with surface immobilized GST-4X. In contrast, preincubation of hTBPc with 4X peptide completely abolished the interaction. Additional experiments showed that the 32-mer, but not the 16-mer,

TABLE 1 There is a synergistic increase in affinity between hTBPc in solution and surface-bound GST-2X when the density of immobilization is increased from 3.8% to 5.7%

	Protein Immobilized	Mass Immobilized (RU)	Protein in Solution	Mass Captured (RU)	Ratio Captured/ Immobilized
Low NTA	GST-2X	1186	hTBP [124 nM]	5	0.004
Density	GST-4X	1060	hTBP [124 nM]	448	0.423
High NTA	GST-2X	2080	hTBP [124 nM]	550	0.264
Density	GST-4X	2516	hTBP [124 nM]	1254	0.498

Low (3.8% NTA) then high (5.7% NTA) density SAMs were docked in an SPR device. Histidine-tagged GST-2X and GST-4X fusion proteins (0.3 mg/ml) were separately immobilized on individual flow cells of the SAMs. The mass of the immobilized species is recorded in resonance units (RU), where 1000 RU = 1 ng protein/mm^2. One RU results from a net change of 1/10,000 of a degree in the angle of minimum reflectance (off the differential dielectric interface) of the sensing wave. hTBPc [124 nM] was then injected over the derivatized surfaces. The mass of the captured analyte was obtained by taking the difference between RU values recorded 10 s before and 25 s after the injection. When GST-2X was immobilized at low density it was not able to bind hTBP. However, when immobilized at slightly higher density, a high-affinity interaction resulted. The stoichiometry of surface immobilized GST-4X binding to hTBPc was relatively constant but, notably, twice that of GST-2X binding to hTBPc, which reinforces the idea that two 2X ligands bind one hTBPc molecule.

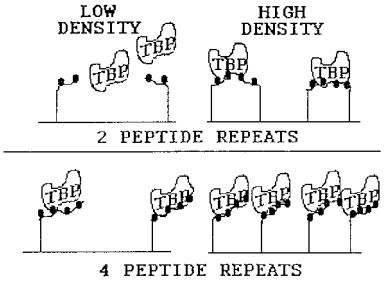

FIGURE 3 The binding of target protein TBP was measured, by SPR, as a function of peptide surface density. A series of NTA-SAMs were generated to display peptides at low to high density. When two tandem repeats of the minimal activation peptide (GST-2X) were displayed at low density (1.3–3.8%), human TBPc did not bind to the surface. In contrast, more dense GST-2X surfaces (5.7–11.4%), bound significant amounts of human TBPc. Fusion proteins bearing four tandem repeats of the minimal activation peptide (GST-4X) bound hTBPc whether the peptides were displayed at low or high density. The stoichiometry of the interaction was a constant, independent of the immobilization density. Notably, at corresponding surface concentrations, GST-2X bound half as much hTBPc as GST-4X, suggesting that two 2X modules immobilized at close proximity to each other (high density) simultaneously contact one hTBPc molecule.

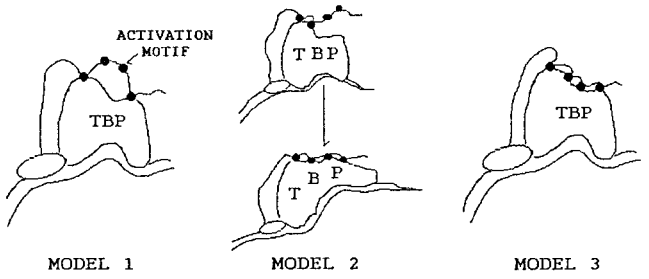

FIGURE 5 Experiments were designed to discriminate among three possible mechanistic models to explain how reiterated peptide activation motifs synergistically effect transcription of a nearby gene. *Model 1:* two connected peptide motifs must be positioned such that they can simultaneously bind to quasi-identical sites on TBP. The bivalent, high-affinity interaction would keep the general transcription factor tethered near the start site of transcription awaiting other steps in the transcriptional activation process. *Model 2:* the binding of one or two peptide activation motifs causes a conformational change in TBP. The allosteric effect enhances the subsequent binding of additional peptide motifs and a high-affinity interaction results. *Model 3:* a high-affinity interaction occurs between the peptide repeats and TBP, but rather than resulting from a "bivalent" interaction or an allosteric effect, it results from the simple summation of multiple interactions between TBP and the entire length of the activation peptide.

peptide also blocked the binding of hTBPc to high-density GST-2X surfaces, again demonstrating that GST-2X, immobilized at high density, behaves like GST-4X.

The competitive inhibition experiments tabulated in Table 2 argue against the allosteric effect model but are consistent with Models 1 and 3. The question is, does the increased binding energy of the hTBP-4X interaction result from the cumulative effect of multiple bonds along the length of the peptide or from the synergistic effect of two minimal motifs simultaneously binding to the target molecule, with the intervening amino acids merely serving as a tether between the two? A synthetic 31 amino acid peptide consisting of two minimal motifs (DFDLDMLG) separated by a flexible linker [$(Ser_4\ Gly_1)_3$] was generated. This peptide, 1X-linker-1X, when preincubated with hTBP (under the same conditions described above) inhibited by 83% the complex's ability to bind to surface-immobilized GST-4X (see Table 2). These results reinforce the premise of Model 1 and imply that the enhanced strength of binding between hTBP and the 4X peptide is due to a synergistic effect caused by two connected minimal activation motifs simultaneously binding to two separate and discrete sites on hTBP. One may also infer, from the last experiment, that the interaction between minimal activation motifs and hTBP is specific.

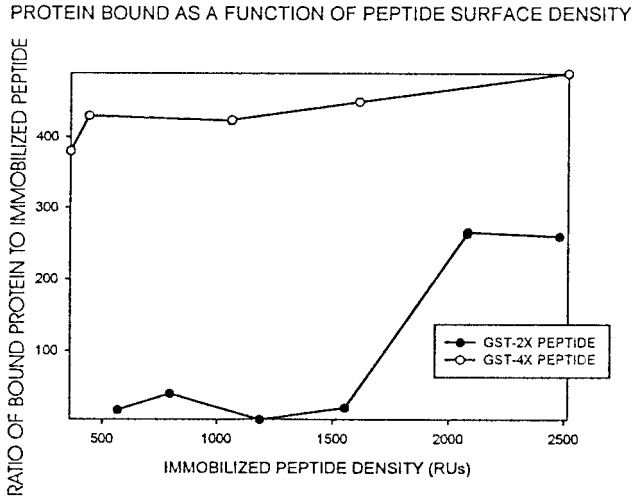

FIGURE 4 The binding of hTBPc to surface immobilized GST-2X is a nonlinear function of the surface density of the peptide. His-tagged peptides were separately immobilized on SAMs presenting NTA over a wide range of surface densities. SPR was used to quantitate the amount of target protein, hTBPc, that bound to each surface. The mass ratios of captured hTBPc to surface immobilized peptide (GST-2X or -4X) was plotted as a function of peptide concentration. The binding of hTBPc to GST-4X (dashed - - line) is roughly constant over the range of surface peptide densities. However, the binding of hTBPc to GST-2X (solid—line) approximates a step function of GST-2X surface concentration.

The kinetics of the surface interactions were compared to analogous interactions in solution. A series of equilibrium inhibition experiments were performed to characterize the solution interactions between hTBPc and 2X or 4X peptides. Aliquots of hTBPc, [124 nM], were mixed with increasing amounts of synthetic 2X or 4X peptide, then incubated at 4° for 1 h before injection over GST-4X surfaces. Titration curves (Fig. 6) yield an IC_{50} of 370 nM for the 4X peptide and 90 μM for the 2X peptide binding to hTBPc. In summary, the 4X peptide binds hTBPc ~250 times better than the 2X peptide. We propose that this is the relative difference between monovalent and bivalent binding of hTBPc. The interaction between the 4X peptide and hTBPc in solution is ~20 times weaker than the comparable surface interaction where diffusion is limited.

TABLE 2 Competitive inhibition experiments show that 2X ligands behave very differently in solution than when surface is immobilized and that reiterated minimal activation motifs effectively compete for the same binding site(s) on hTBP as the parent protein

Protein Immobilized	Mass Immobilized (RU)	Protein in Solution	Mass Captured (RU)	Ratio	Inhibition
GST-4X	358	$hTBP_c$ alone	230	0.642	0%
GST-4X	438	$hTBP_c$ + 2X peptide	322	0.735	0%
GST-4X	571	$hTBP_c$ + 4X peptide	0	0.000	100%
GST-2X	2080	$hTBP_c$ alone	550	0.264	0%
GST-2X	2141	$hTBP_c$ + 2X peptide	556	0.259	2%
GST-2X	1930	$hTBP_c$ + 4X peptide	51	0.026	91%
GST-4X	923	hTBP alone	600	0.650	0%
GST-4X	1094	hTBP + 1X-linker-1X	122	0.111	83%
Gal-4-VP16	732	hTBP alone	483	0.659	0%
Gal-4-VP16	727	hTBP + 4X peptide	36	0.049	93%

Histidine-tagged GST-4X or GST-2X were separately immobilized on NTA-SAMs docked in a Biacore SPR instrument. hTBPc (residues 155–335) or hTBP (full length) was pre-incubated at high concentration [35 μM] with either buffer, a synthetic 2X peptide (X = DFDLDMLG) at 1:4 stoichiometry, a 4X peptide at 1:2 stoichiometry, or a 1X-linker-1X peptide (DFDLDMLG-$((Ser)_4Gly_1)_3$-DFDLDMLG) at 1:2 stoichiometry for 1 h at 4°C. Just prior to injection over the derivatized surfaces, the preincubation mixtures were diluted such that the final hTBP concentration was 124 nM. The synthetic 4X and 1X-linker-1X peptides blocked the interaction of hTBP with surface-immobilized ligands but 2X peptides were not inhibitory. Histidine-tagged Gal-4 (1–147) + VP16 (413–490) were similarly immobilized on NTA-SAMs. hTBP was preincubated, as described above, with either buffer or 4X peptide, then diluted and injected over the VP16 presenting surfaces. The 32 amino acid 4X peptide effectively blocked the interaction of hTBP with the 78 amino acid VP16 activation domain.

The physiological relevance of the interaction between hTBP and the reiterated minimal motifs was investigated. It has been argued that the widely observed in vitro interactions between TBP and activation domains are artifacts resulting from a nonspecific interaction between TBP's basic DNA-binding region and the acidic peptides. To rule out this possibility, N-terminally His-tagged hTBP was immobilized on NTA-SAMs, then separately incubated with either 1) TATA sequence DNA; or 2) DNA that did not contain a hTBP recognition sequence. GST-4X was then injected over the derivatized surfaces. DNA that did not contain a TATA sequence did not bind to the immobilized hTBP significantly. DNA containing a TATA sequence bound to immobilized hTBP with approximate 1:1 stoichiometry but was in no way inhibitory to the subsequent binding of GST-4X (Fig. 7). In fact, hTBPc complexed by its cognate DNA bound roughly twice as much GST-4X as the uncomplexed hTBPc. This result is consistent with the observation that hTBPc exists as a dimer that is disrupted upon DNA binding (Taggart and Pugh, 1996). The binding of an activating region does not seem to disrupt hTBPc dimerization.

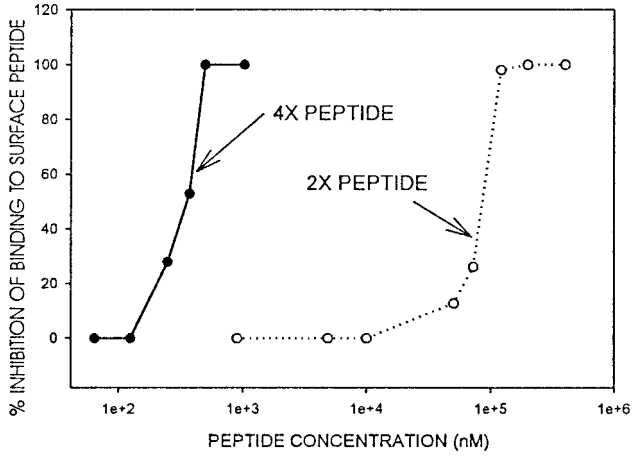

FIGURE 6 Titration curves, summarizing competitive inhibition experiments, yield IC_{50}s that show the 4X peptide binds hTBPc 250 times tighter than the 2X peptide. In order to quantitate the solution kinetics of hTBPc binding to synthetic 4X peptides (four tandem repeats of DFDLDMLG) or 2X peptides (two repeats), aliquots of hTBPc [124 nM] were incubated with increasing concentrations of either peptide at 4°C for 1 h. The mixtures were then separately injected over identical SAM that were pre-bound with GST-4X. Percent inhibition is plotted against the concentration of the blocking peptide in solution. Zero percent inhibition was taken to be the amount of hTBPc that bound to GST-4X surfaces when it was incubated with buffer alone. Background levels of binding were determined by injection of protein mixtures over naked GST surfaces. An IC_{50} of 370 nM and 90 μM describe the equilibrium kinetics of hTBPc binding to 4X and 2X peptides, respectively.

A competitive inhibition experiment was performed to determine whether the 4X peptide could block the interaction between hTBP and the native activation domain of VP16. A His-tagged Gal-4(1–147) + VP16(413–490) fusion protein was immobilized on NTA-SAMs. hTBP was incubated with buffer or 4X peptide, then injected over VP16 derivatized surfaces. The last two lines of Table 2 show that preincubation of hTBP with the 4X peptide (32 amino acids) completely abolished the hTBP-VP16 (78 amino acids) interaction. This result is consistent with the idea that minimal activation motifs recognize the same binding site(s) on hTBP as the parent activator.

CONCLUSION

SAMs were used to form biospecific rigid, nanoscale probe arrays of known surface density and then used to determine the number of binding sites on a target molecule and an

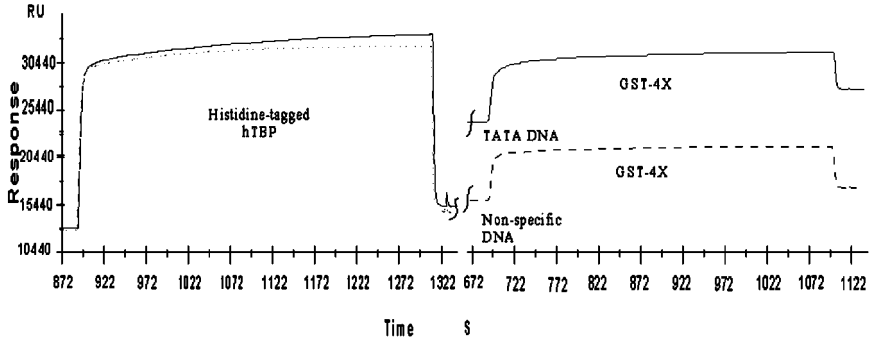

FIGURE 7 TATA sequence DNA bound to hTBP does not inhibit the hTBP/GST-4X interaction. N-terminally His-tagged hTBP was bound to NTA-SAMs and the mass of bound protein was quantitated and recorded by a BIAcore SPR instrument. The SAMs, bound with hTBP, were then removed from the instrument and separately incubated at RT for 15 min with solutions containing equal mass amounts of either DNA bearing the hTBP TATA recognition sequence or random-sequence DNA (150 mM NaCl; 50 nM DNA). The SAMs were then washed in running buffer and re-docked in the SPR instrument. The increase in absolute RU of the baseline indicated that the TATA sequence DNA bound to surface immobilized hTBP with roughly 1:1 stoichiometry while the random DNA bound only nonspecifically. Protein plugs of GST-4X were separately injected over these surfaces; the presence of DNA, bound nonspecifically or specifically, was not inhibitory to the subsequent binding of GST-4X to hTBP. Additionally, the measured association and dissociation rates, which were not affected by DNA-binding, were identical to those measured with GST-4X bound to the SAM and TBP in solution.

approximate distance between sites. This approach is not hampered by the vagaries of secondary or tertiary structures that would be encountered by using DNA or peptide spacers to determine distances between active sites. We used SPR to show that the avidity between TBP, in solution, and surface immobilized peptides was a nonlinear function of peptide surface density. Peptides immobilized on a 3.8% NTA-SAM were not able to bind hTBP, while peptides presented on a 5.7% NTA-SAM bound TBP with nanomolar affinity. These findings are consistent with the idea that this large increase in binding strength marks the transition between mono and bivalent binding of the target protein. Individual eight-amino acid minimal activation motifs separated by a 15-amino acid flexible linker bound hTBP nearly as well as four tandem repeats of the motif, leading to the conclusion that hTBP has at least two discrete sites capable of simultaneously interacting with the eight amino acid motif. Calculations based on an assumed Poisson distribution of NTA in the SAM indicate that the surfaces that did not bind hTBP (3.7% NTA) presented peptides an average distance of 29 Å apart, while peptides in denser arrays (5.7% NTA) that bound hTBP with high avidity were, on average, 23 Å apart. The crystal structure of hTBPc has been solved (Nikolov et al., 1996). The peptide consists of two imperfect repeats that form a two-domain saddle-shaped DNA-binding protein with twofold intramolecular symmetry. TBP binds DNA with the concave underside of its "saddle" shape. The general transcription factor TFIIB binds near the TBP/DNA complex at the downstream end, leaving the convex "seat" of the saddle available for other intermolecular interactions. Quasi-identical structures composed of basic helices and β sheets flank the seat of the saddle. Mirror image helices H2 and H2′ are separated by distances on the order of 20 Å. It is conceivable that the minimal activation motifs, described herein, simultaneously bind to twofold related pseudo-identical recognition sites that may be separated by ~23 Å.

We imagine that similar schemes can be devised to determine distances between active sites on other bivalent molecules or complexes. Of particular interest are dimeric hormone receptors whose signaling activity depends on its association state. Detailed knowledge of distances between active sites would allow for the rational design of agonist or antagonist drugs.

The author is grateful to the Whitesides laboratory for useful discussions and for providing gold substrates, Masafumi Tanaka for plasmids and proteins, the Burley laboratory for hTBPc, and Mike Carey's laboratory for His-tagged hTBP. Thanks to Bob Staszewski for helping with Poisson theory and Jeff Hoch for stimulating scientific discussions.

This work was supported by the Biophysics Program Grant NRSA 5T32GM-07598-18 and National Institutes of Health Grant GM-32308.

REFERENCES

Baleja, J. D., R. Marmorstein, S. C. Harrison, and G. Wagner. 1992. Solution structure of the DNA-binding domain of Cd2-Gal4 from *Saccharomyces cervisiae. Nature.* 356:450–453.

Bamdad, C., G. Sigal, J. Strominger, and G. M. Whitesides, inventors; The President & Fellows of Harvard College, assignee. 15 April 1997. Molecular recognition at surfaces derivatized with self-assembled monolayers. U.S. patent 5,620,850.

Bamdad, C. 1997. Surface plasmon resonance for measurements of biological interest. *Current Protocols in Molecular Biology.* 20.4.1–20.4.12.

Brent, R., and M. Ptashne. 1985. A eukaryotic transcriptional activator bearing the DNA specificity of a prokaryotic repressor. *Cell.* 43: 729–736.

Burley, S. K., and R. G. Roeder. 1996. Biochemistry and structural biology of transcription factor IID (TFIID). *Annu. Rev. Biochem.* 65:769–799.

Daniels, P. B., J. K. Deacon, M. J. Eddowes, and D. G. Pedley. 1988. Surface plasmon resonance applied to immunosensing. *Sens. Actuators.* 16:11–18.

Ellenberger, T. E., C. J. Brandl, K. Struhl, and S. C. Harrison. 1992. The GCN4 basic-region-leucine zipper binds DNA as a dimer of uninterrupted helices: crystal structure of the protein-DNA complex. *Cell.* 71:1223–1237.

Hochuli, E., H. Dobeli, and A. Schacher. 1987. New metal chelate adsorbent selective for proteins and peptides containing neighboring histidine residues. *J. Chromatogr.* 411:177–184.

Hori, R., S. Pyo, and M. Carey. 1995. Protease footprinting reveals a surface on transcription factor TFIIB that serves as an interface for activators and coactivators. *Proc. Natl. Acad. Sci. U.S.A.* 92:6047–6051.

Ingles, J. C., M. Shales, W. D. Cress, S. J. Triezenberg, and J. Greenblatt. 1991. Reduced binding of TFIID to transcriptionally compromised mutants of VP16. *Nature.* 351:588–590.

Jencks, W. P. 1981. On the attribution and additivity of binding energies. *Proc. Natl. Acad. Sci. U.S.A.* 78:4046–4050.

Lee, W. S., C. C. Kao, G. O. Bryant, X. Liu, and A. J. Berk. 1991. Adenovirus E1A activation domain binds the basic repeat in the TATA box transcription factor. *Cell.* 67:365–376.

Liedberg, B., C. Nylander, and I. Lundstrom. 1983. Surface plasmon resonance for gas detection and biosensing. *Sens. Actuators.* 4:299–304.

Lin, Y. S., M. Carey, M. Ptashne, and M. R. Green. 1990. How different eukaryotic transcriptional activators can cooperate promiscuously. *Nature.* 345:359–361.

Löfås, S., and B. Johnsson. 1990. A novel hydrogel matrix on gold surfaces in surface plasmon resonance sensors for fast and efficient covalent immobilization of ligands. *J. Chem. Soc., Chem. Commun.* 1526–1528.

Marmorstein, R., M. Carey, M. Ptashne, and S. C. Harrison. 1992. DNA recognition by Gal4: structure of a protein/DNA complex. *Nature.* 356:408–414.

Nikolov, D. B., H. Chen, E. D. Halay, A. A. Usheva, K. Hisatake, D. K. Lee, R. G. Roeder, and S. K. Burley. 1995. Crystal structure of a TFIIB-TBP-TATA element ternary complex. *Nature.* 377:119–128.

Nikolov, D. B., H. Chen, E. D. Halay, A. Hoffmann, R. G. Roeder, and S. K. Burley. 1996. Crystal structure of a human TATA box-binding protein/TATA element complex. *Proc. Natl. Acad. Sci. U.S.A.* 93: 4862–4867.

Nuzzo, R. G., L. H. Dubois, and D. L. Allara. 1990. Fundamental studies of microscopic wetting on organic surfaces. I. Formation and structural characterization of a self-consistent series of polyfunctional organic monolayers. *J. Am. Chem. Soc.* 112:558–569.

Pale-Grosdemange, C., E. S. Simon, K. L. Prime, and G. M. Whitesides. 1991. Formation of self-assembled monolayers by chemisorption of derivatives of oligo (ethylene glycol) of structure $HS(CH_2)11(OCH_2CH_2)_mOH$ on gold. *J. Am. Chem. Soc.* 113:12–20.

Parvin, J. D., R. J. McCormick, P. A. Sharp, and D. E. Fisher. 1995. Pre-bending of a promoter sequence enhances affinity for the TATA-binding factor. *Nature.* 373:724–727.

Sheldon, M., and D. Reinberg. 1995. Tuning up transcription. *Curr. Biol.* 5:43–46.

Sigal, G., C. Bamdad, A. Barberis, J. Strominger, and G. M. Whitesides. 1996. A self-assembled monolayer for the binding and study of histidine-tagged proteins by surface plasmon resonance. *Anal. Chem.* 68: 490–497.

Taggart, A. K. P., and B. F. Pugh. 1996. Dimerization of TFIID when not bound to DNA. *Science.* 272:1331–1333.

Tanaka, M. 1996. Modulation of promoter occupancy by cooperative DNA binding and activation-function is a major determinant of transcriptional regulation by activators in vivo. *Proc. Natl. Acad. Sci. U.S.A.* 93: 4311–4315.

Tanaka, M., and W. Herr. 1994. Reconstitution of transcriptional activation domains by reiteration of short peptide segments reveals the modular organization of a glutamine-rich activation domain. *Mol. Cell. Biol.* 14:6056–6067.

Triezenberg, S. J. 1995. Structure and function of activation domains. *Curr. Opin. Genet. Dev.* 5:190–196.

Xiao, H., J. D. Friesen, and J. T. Lis. 1995. Recruiting TATA-binding protein to a promoter: transcriptional activation without an upstream activator. *Mol. Cell. Biol.* 15:5757–5761.

Ulman, A., 1966. Ultrathin Organic Films. Academic Press, San Diego, CA.